Journal of Earth Science & Climatic Change

Babazadeh, J Earth Sci Clim Change 2022, 13:11

Research Article Open Access

Estimation the Influence of Dynamics of Land Surface Temperature on Delhi Urban Heat Island

Mina Babazadeh*

Department of Regional Development, Jawaharlal Nehru University, New Delhi, India

Abstract

Land surface temperature LST, land surface changes, vegetation cover and other land parameters are a significant dynamic in worldwide climate change researches structure. Land surface changes have brought essential changes on to the vegetation cover for cities, as well as urban heat-trapping and raising temperature regimes resulting in unsustainable environments. This study tries to look at urban heat islands issues in Delhi based on thermal remote sensing Landsat data. Thermal Infrared (TIR) Landsat 5, 7 and 8 proved that it is possible observing land temperature which has been touched by different microclimate conditions in the cities. Satellite data has a vital role in the land observation of the surface changes across the world, mainly wherever necessary knowledge isn't accessible for such observations. This study used Landsat 5, 7 and 8 images to observe unique patterns of land surface temperature and heat island growth in Delhi during (1996, 2003, 2010 and 2017). This study proved that the central part of Delhi facing a low temperature, which is starting from 28°C for and 49°C for suburban part of Delhi which has been covered by rock and new growth settlements areas. Moderately, a low temperature has recorded in vegetation cover and water bodies in the middle part of the Delhi. A central part covered by enough density of vegetation cover and tree cover. The higher temperature has recorded for high dance build-up areas ranges between 48°C and 52°C. The results show that urban heat island growth has transferred from the central part of the city to surrounding areas from 1996-2017. The heat-trapping in the South, South West and North West part of the city due to the high concentration of building and grown societies and industrial units over Delhi caused an It recommended that development authority should consider environmental concern before planning industrial land use and urban growth must be regulated and perpetually monitored.

Keywords: Heat trap; Urban heat island; Land surface temperature; NDBI

Introduction

The Land Surface Temperatures (LST) defines the temperature emitted from the Land Surface (LS) because of different activities associated with the LS. Human activities have played a crucial position in urban transformation, *viz.* change of Land Use (LU) for different functions that influence local climate, air circulation, ground land modification in the surface energy resources, discharge patterns with heat transfers. The growing construction usage of Low reflective materials to make buildings removing vegetation cover and emission from numerous rocky area of various sources have determined that LST is one of the vital parameters concerning the exchange of long-wave radiation and turbulent heat fluxes at the surface-atmosphere interface in Delhi region. Amplified LST in city sacks in compared through surrounding areas to the rise in cement surfaces thought as Urban Heat Island (UHI) development. UHI formation and heating impact in an urban area which is a property related to the urban and land transformation that is the vital essential concentration in scientific disciplines. It is a result of a UHI signal provides approaching about land cover and land use changes happening because of individual activities. It casts a strict contact on human health, system performance and local climate at the end of our days. All the adverse effects happen as results of reduction in heat transformation flux and additionally increase in sensible heat fellow during a geographical region at urban areas. Hence, changes in heat ratio occur by all the indicators. Which is brings temperature a differential characteristic that was referred as Urban Heat Island (UHI) by Manley in 1958, and later on other studies started to differentiate on air temperature plus surface temperature estimation. Satellite images are the best prime basis of data to mark the land surface heat islands. Generally, with the help of land surface temperature maps can be drawn a heat time series at a hot spot across cities. Here, remote sensing develops different techniques to monitor and capture LST with the help of thermal images at the different satellite which linked to the land surface behaviour at particular areas found that barren land has the high land surface temperature. On the other hand observed that settlements areas strongly linked to high land surface temperature estimated that the extremely high density residential area is under risk of UHI in comparative with medium/less residential settled areas.

Nevertheless, knowing and analysis of different variables which will have an effect on LU/LC and spatial circulation of temperature in the city didn't analyse. During this affiliation, the peculiar built-up distribution of city structures could be an issue which will affect the deviation of the temperature within the urban. Nevertheless, few studies have spoken the correlation among urban Land Cover and Land Use (LU/LC) structure, particular configuration and LST. This research tray to discuss the connection between the land surface temperature characteristic and urban heat-trapping patterns supported by land surface temperature modification of surface characteristics, land use, and land cover patterns and configuration.

***Corresponding author:** Mina Babazadeh, Department of Regional Development, Jawaharlal Nehru University, New Delhi, India; E-mail: mina58_ssf@jnu.ac.in

Received: 16-Sep-2020, Manuscript No. JESCC-20-19272; **Editor assigned:** 21-Sep-2020, PreQC No. JESCC-20-19272(PQ); **Reviewed:** 05-Oct-2020, QC No. JESCC-20-19272; **Revised:** 18-Nov-2022, QI No. JESCC-20-19272; Manuscript No. JESCC-20-19272(R); **Published:** 16-Dec-2022, DOI: 10.4172/2157-7617.1000648

Citation: Babazadeh M (2022) Estimation the Influence of Dynamics of Land Surface Temperature on Delhi Urban Heat Island , India. J Earth Sci Clim Change 13:648

The current study tries to look for the relation between the land characters, for example, NDBI and NDVI indicators and LST on heat-trapping over (1996, 2003, 2010 and 2017) years. This study tried to predicate the correlation between abstraction integration values of land surface with UHI within the study area. The final results by evaluating the reduction of UHI impact associated formation will help to a higher understanding of the spatiotemporal patterns of urban heat island and its associations with and urban characters ices, which has necessary implications for several urban planning and also this work will give necessary implications for the urban land use management and facilitate decision-makers in urban policy, environmental coming up with and design.

Remote sensing and heat-trapping

Monitor and forecast of future LST conditions and changes need the correct and fast acquisitions which is information regarding the extent of the changes. Prediction algorithms that measure right predict LST for sensitive info regarding the climate system. Such info can change Delhi region to know and adaptation methods and policies in urban coming up with and different way that decreases the UHI impact. This i nfo c an be accessible b y e xploitation r emote-sensing knowledge. Over the years, some analysis efforts dedicated to LST prediction. For instance expected future urban surface temperatures exploitation with medium resolution satellite with the hel of Salisbury metropolitan town, Zimbabwe modelled LST exploitation by remote sensing in Turkey, whereas LST below cloudy conditions on Cauvery geographic region. Prediction of future surface temperatures supported by land elements analysis is an essential key to mitigating UHI impacts. Many studies utilised land cover indices to the future distribution of LST utilized (NDVI) to increase future LST estimation. In their study, the authors used a single regression model and random mathematician model to predict LST. They investigate that NDVI is the best predictor or element for LST. Studies show that NDVI could be a low indicator of land surface temperature analysis tried the potential of associate degree assortment of vegetation and non-vegetation indices to foresee land surface temperature. Therefore, the objectives of this study will measure to investigate the link between LST with UHI and NDBI and NDVI conditions.

Study area

National Capital Territory (NCT) of Delhi is bounded by the Indo-Gangetic alluvial plains in the North and East, by the Thar Desert in the West and by Aravalli hill ranges in the south. The terrain of NCT of Delhi is flat in general except for a low NNE-SSW trending ridge that is considered an extension of the Aravalli hills of Rajasthan. The ridge may be said to enter NCT of Delhi from the SW (Figure 1). The eastern part of the ridge extends up to Okhla in the south and disappears below Yamuna alluvium in the NE on the right bank of the river. NCT of Delhi is one of the largest metropolitan cities in the world. The population density is 11,297 P/km^2, the highest in the country. The average elevation is 200-256 m above mean sea level. The Yamuna River flows across Delhi from the north-east to south-east direction. The weather is most extreme. The April temperature ranges from 25°C to 45°C, and the winter temperature (December to January) ranges from 22°C to 5°C. The August month experiences the highest average rainfall in a year. Delhi also faces severe fog and smog formation during winter in Figure 2.

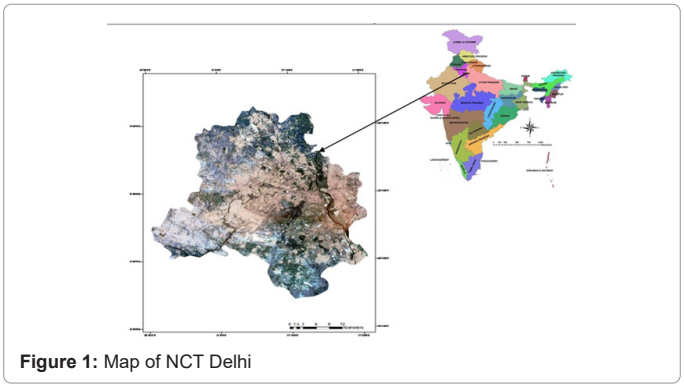

Figure 1: Map of NCT Delhi

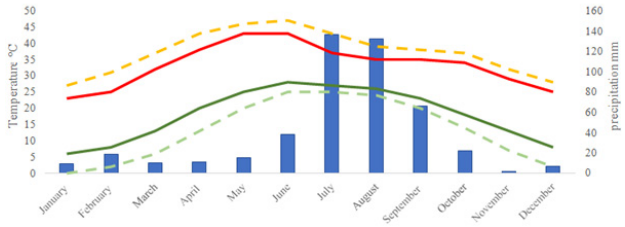

Figure 2: Average Monthly Temperature and precipitation in Delhi (1996-2017). **Note:** ( ) Perception; ( ) Mean maximum tem; ( ) Mean minimum tem; () Hot days; ( ) Coldest days.

Data Set

In this research is investigated correlation LST-with land elements for Delhi city using remotely sensed images. The presentation focused on the thermal remote sensing application of Landsat satellite images. Landsat 5 TM/7 ETM/8 OLI, all data were used in this study for modeling and the details of the user data given in Table 1.

Nr. Crt	Path	Row	Date	Cloud cover (%)	Satellite
1	182	27	01.04.1996	0	Landsat 5
2	182	27	02.04.2003	0	Landsat 7
3	182	27	09.04.2010	0	Landsat 5
4	182	27	22.04.2017	0	Landsat 8

Table 1: Details of landsat data retrieved.

Data processing

Image pre-processing of land sat image: The purpose of image pre-processing is to build all of the remote sensing images comparables so that images can regard as taking in the same environmental circumstances with the same sensors. To fill up the gaps with Landsat 7 images, a dedicated toolbox of Arc Map 10.1 used. Pre-processing of Landsat 5, 7 and 8 data stages correspond to that process that prepares images for subsequent analysis that attempts to compensate/correct for systematic errors. Generally, atmospheric and radiometric corrections are considered as most significant pre-process steps in the processing of satellite images, as well as evaluation of LST. For radiometric corrections, the Digital Numbers (DNs) of all pixels in the image were converted to spectral radiance using the data in the image header file and based on equation 1.

$$ToA_r = \frac{R_{Max-}R_{Min}}{Q_{Max-}Q_{Min}} * (DN - Q_{\min}) + R_{Min} \quad (1)$$

Digital Numbers (DN) is the identified digital number per pixel, and Top of Atmosphere Radiance (ToAr) is the planned value per each cell. L_{Max} and L_{Min} are the calibration constants of the sensor, equal to the max and min values of the spectral radiance (in W/m2/sr/mm) detectable for each band, by the sensor Landsat TM.

Although the primary geometric corrections on the Landsat products, to eliminate possible errors in the image of the study area, it geometrically rectified with national topographical maps at a scale of 1:25,000. The improvement method performed by the first- order Polynomial model using nearest neighbor re-sampling method RMSE designed using to make sure the accuracy assessment of geometric correction. This factor calculates the difference among observed values and predicted principles as shown in equation 2.

$$RMSE = \sqrt{\frac{1}{N}\sum_{i=1}^{N}(X_i - X_i)^2} \quad (2)$$

The RMS error of the image approximate at 0.03.

Satellite image processing

Normalised Difference Vegetation Index (NDVI): This index is a numerical indicator, can be used for visible and Near-Infrared (NIR) bands of the electromagnetic spectrum which was adopted to analyse remote sensing dimensions and consider whether the objectives being pragmatic contains fresh green vegetation cover or not. The NDVI algorithm subtracts the red reflectance values from the Near-Infrared (NIR) and divides it by the sum of those bands as shown in equation 3.

NDVI=NIR-VIR/NIR+VIR (3)

In theory, the value of this index is variable in the range of (+1 and −1). The value of NDVI for dense vegetation usually differs from 0.3 to 0.6, and negative values indicate the clouds, snow covers and water. There have been many studies on the relationship between LST and vegetation cover by analysing the values of NDVI and surface temperature in which the critical role of NDVI and its variations on LST map at different LU/LC classes emphasised. The present study also examined the correlation between changes in LST and vegetation cover measured by NDVI.

Land surface temperature extraction

Landsat 5 TM: Following the result of the satellite image brightness, using the technique to develop for the sensors with only one thermal bond, the LST was computed based on (equations 4-6).

$$Ts = \Upsilon\{\varepsilon^{-1}(\varphi_1 L_s + \varphi_3\} + \delta \quad (4)$$

$$\Upsilon = \{\frac{C_2 L_s}{T_b^2}(\frac{\lambda^4}{C_1}L_S + \lambda^{-1})\}^{-1} \quad (5)$$

$$\delta = \Upsilon^{L_S} + T_S \quad (6)$$

In which (Ts) is the land surface temperature (LST), (λ) is the effective wavelength, which regarded to be 11.5 μm this research, (ε) is surface emissivity, (C1 and C2) is constant values of 1.19104 × 108 μ 4 m^{-2} sr^{-1} and 14387.7 μm K, respectively, and (ϕ1, ϕ2, ϕ3) is atmospheric functions that calculated using Equations (7-9) and the amount of water vapor in the atmosphere at the time of imaging. The average water vapor in the study area estimated at 0.748.

$$\varphi_1 = 0.14714W^2 - 0.15583W + 1.1234 \quad (7)$$

$$\varphi_2 = 1.1836W^2 - 0.373607W + 0.52894 \quad (8)$$

$$\varphi_3 = -0.04554W^2 - 1.8719W + 0.39071 \quad (9)$$

Landsat 7 ETM

The extraction of LST information from Landsat 7 ETM+ conducted using an algorithm that has mentioned in the Handbook of Landsat 7 ETM+. This algorithm consists of series of sequences that must under taken starting from changing the pixel principles into radiance values, converting the radiance into temperature brightness, and in conclusion converting the temperature brightness into kinetic temperature (LST). The algorithms used exposed in Equations (10 and 11) below.

$$L\lambda = (\frac{(LMAX\lambda - LMIN\lambda)}{QCALMAX - QCALMIN}) \times (QCAL - QCALMIN) + LMIN\lambda \quad (10)$$

$$T = K2 / In(K1 / L\lambda + 1) \quad (11)$$

Where L MAX and L MIN are spectral values contained in the meta-data of Landsat images, the calibration values of pixels for $QCAL_{Max}$ and $QCAL_{MIN}$ can be found from Landsat data meta-data. K1 and K2 are predetermined constants values and Lλ is the spectral radiance value of the image. The final result from these algorithms is surface temperature brightness information.

Landsat 8 OLI/TIRS

The LST extraction in Landsat 8 OLI/TIRS used a Split Windows Algorithm (SWA) algorithm that developed. This algorithm previously applied for LST derivation from NOAA AVHRR weather images. The confront in this algorithm is that water vapour and emissivity principles need to verify before the implementation of the algorithm (Equation 12).

$$T_s = A_0 + A_1 * T_{10} - A_2 * T_{11} \quad (12)$$

T_{10} and T_{11} are the results of temperature brightness which obtained from band ten and band 11 of Landsat 8. The values of A_0, A_1 and A_2 are the results of decreasing value of the information obtained from the communication atmospheric water vapor and individual emissivity assessment. As a final point, spectral radiances be transformed into satellite brightness temperature by the following association that is similar to the Planck equation with two free parameters equation 13. In fact, to generate surface temperatures, the surface leaving radiance needs to be transformed to the surface leaving temperature. Radiance to temperature is accessible by the Landsat specific estimate of the plank curve equation;

T=K2/In(K1/Lλ+1) (13)

Where;

- T=Effective at-satellite temperature in Kelvin
- K1=Calibration constant 1 (watts/meter squared*ster*μm) (666.09)
- K2=Calibration 2 (Kelvin) (1282.71)

Lλ=Spectral radiance (watts/meter squared*ster*μm)

It is where you use the K1 and K2 inputs. The equation we will be using functions to use is (Table 2).

Specific thermal conversion constant	Landsat5(TM)	Landsat7(ETM)	Landsat8(TIRS)
K1 (BAND_6)	607.76	666.09	-
K2 (BAND_6)	1260.56	1282.71	-
K1 (BAND_10)	-	-	774.89
K2 (BAND_10)	-	-	1321.08
K1 (BAND_11)	-	-	480.89
K2 (BAND_11)	-	-	1201.14

Table 2: The metadata of Landsat 5,7and 8 band-specific thermal conversion constants.

The last products from these processes were separate temperature datasets of remotely sensed land surface temperatures from each of the entire images, as well as the cities and surrounding areas of the corridor study region. The brightness temperatures from TM, ETM band six and TIRS band ten and11 thermal then used to analyse the LST using the Sobrino equation (Equtation14)

$$LST = \frac{BT}{1} + W \times ((\frac{BT}{P}) \times In(e)) \qquad (14)$$

Where:

T_s=Land surface temperature

BT=At-sensor brightness temperature (K) and p=143800

W=Wavelength of emitted radiance (11.5um)

ln (e)=Log of the spectral emissivity value

Estimation of urban heat Island

In this study, the UHI analyses in the following equations:

$LST > \mu + 0.5 \times \delta$ referred to UHI area

$0 < LST \leq \mu + 0.5 \times \delta$ denoted non-UHI or rural area

Where μ is indicating and δ is the Standard Deviation (SD) of LST in the study area. The intensity of UHI identified as the differential temperature linking the average temperature of UHI areas and rural area UHI intensity was understood to be as the average temperature difference between urban and rural areas. The average temperature of the urban area and rural area was 49.6°C and 25.9°C, on 2000 and 47.7°C and 26.2°C respectively. So, the heat island intensity in Delhi was 9.7°C, and the heat island effects were evident during 2000. For this study, we used the thermal variance index to analyse the UHI spatial distribution on Delhi 1996-2017. Also, the thermal variance index (HI) is defined as follows (Equation15)

$$HI = T_s - T_{mean} / T_{mean} \qquad (15)$$

Where Ts and Tmean defined the land surface temperature and the mean LST of the city, respectively. UHI graded into four degrees in this study. This has been classified in 6 categories: None, weak, middle, strong, stronger and strongest.

Results and Discussion

Land use and land cover classification

The LULC classification in this study has been performed by a supervised classification technique. Five categories have been identified over the research area, namely build-up, agriculture land, green area, barren land and water body shows areal statistics of LU/LC classes. Table 3 demonstrates that the barren land is the main LU/LC category in 1996 and 2010. Water occupies the small percentage of the whole area in Delhi. There is an increase in the build-up while the conflicting tendency can see for barren land and vegetation cover in Delhi. Barren land observed slight decreased during the study period (Table 3).

	1996		2003		2003		2017	
LULC	Area	%	Area (ha)	%	Area (ha)	%	Area (ha)	%
Build-up	330.71	22.01	480.79	32.01	648.45	43.17	547.38	36.43
Agriculture	611.44	40.7	531.33	35.37	507.49	33.79	508.87	33.8
area								
Vegetation	187.48	12.78	235.26	15.66	160.35	10.68	339.62	22.61
Barren land	352.09	23.44	237.58	15.82	176.19	11.73	95.5	6.36
Water Body	1.004	1.07	19.94	1.15	13.53	0.63	12.418	0.8

Table 3: Area statistics of LULC classes for 1996, 2003, 2010 and 2017.

Therefore, the overall accuracies for the years 1996, 2003, 2010 and 2017 were 75.00%, 84%, 83% and 87% respectively. Build-up area and vegetation cover got the maximum accuracy in all four years. Barren land got the minimum accuracy. The kappa coefficients for the classification images were 0.66, 0.70, 0.75 and 0.79, respectively.

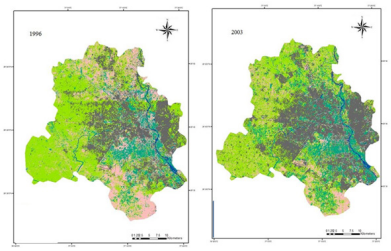

Figure 3: LU/LC map of the study area in 1996 and 2003.

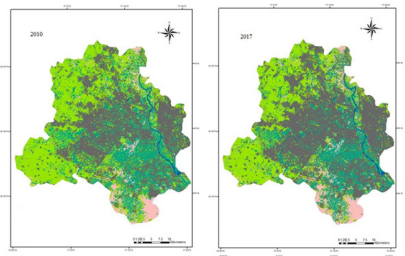

Figure 4: LU/LC map of the study area in 2010 and 2017. Note: ( ) Water body; ( ) Build up; ( ) Vegetation cover; ( ) Agriculture area; ( ) Baren land.

Recognised that barren land has a high impact on land surface temperature. The maximum proportion of barren land was found in South, South-West and North of Delhi, all over the study period, due to the decrease in agricultural land and activities. Also, the appearance

of new built-up areas in South of Delhi and South-West causes' huge decline of 'Delhi ridge', which is a biodiversity enriched zone measured as 'natural lounges' of the city. Another reason is deforestation, loss of natural geomorphologic stream and illegal encroachment along with the great growth of built-up land.

Land surface temperature from landsat images

LST variation maps of 1996, 2003, 2010 and 2017. The LST map prepared from Landsat TM satellite image in April. The temperatures in thesis maps were classified based on a standard deviation of values, and subsequently, areas affected by urban heat island identified. According to the LST maps the surface temperature various between 21.5°C and 49.9°C. At the time of imaging the lowest average temperature was 35°C related to the water bodies and the maximum average temperature was 48°C recorded from bare lands in the study area (Figures 5 and 6).

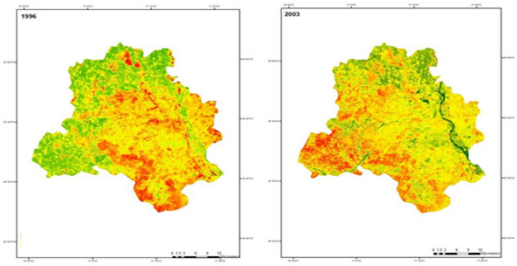

Figure 5: LST of the study area for the years 1996 and 2003.

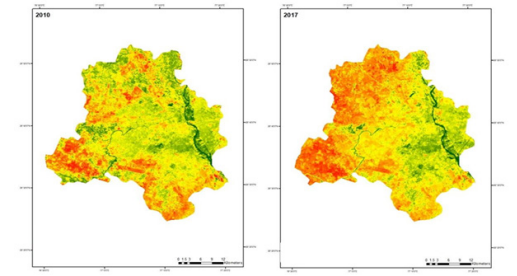

Figure 6: LST of the study area for the years 2010 and 2017 (April).

The mean LST inside each LULC class in the study area. The water body in land use and land cover type got the minimum mean LST values in all four years (18.9°C in 1996, 25.8°C in 2003, 26.8°C in 2010 and 25.3°C in 2017) which is even lower than vegetation cover (19.8°C in 1996, 33 in 2010, 30.5°C in 2010 and 26.3°C in 2017). Build-up got the maximum mean LST values in all four years (21.2°C in 1996, 40.47°C in 2003, 39.2°C in 2010 and 28.6°C in 2017). Build-up area, agriculture area, got the highest mean LST values (17.6°C in 1996, 37.04°C in 2003, 36.5°C in 2010 and 31.2°C in 2017). The mean LST for fallow land is 17.6°C in 1996, 36.2°C in 2003, 36.19°C in 2010 and 29.5°C in 2017. Similarly, the mean LST value for vegetation is 19.8 °C in 1996, 33°C in 2003, 30.5°C in 2010 and 26.3°C in 2017. In this way, vegetation cover and water body received low mean LST values, build up and Agriculture areas received high, and fallow land received average values. The high LST values found in the north-western, southwest and South parts of the city. This portion of the area is characterized by barren land during 1996-2003 and following with a growing population, those areas turn to settlement. The central part of the study area presents the less LST during 2010- 2017, where a high concentration of urban green area and water bodies observe.

Relationship between LST and LU/LC

The association among LST and Land Use/Land Cover (LULC), mainly green cover whose parcelling situation in the research was prove with NDVI, variations in the LST of various LULC modules were considered. Compare the approximate surface temperature values and the LU/LC map exposed the thermal variation in different LU/LC classes. The lowest Surface Temperature (ST) correspond towards the water bodies, and the highest ST was the record in built up area and impervious surfaces such mining industrial area, as well as other man-made coatings Urban Heat Island (UHI) is mainly situate in 3 different areas in Delhi as well as a variety of LULC. The main exaggerated areas are located in North, south west and South region of the Delhi, mining industrial the vast majority of factories, industrial workshops, rocky lands and other related LU, because a chain of mining industrial activities. In other words the common of the region engaged by industrial LU and man-made regions (Figure 7).

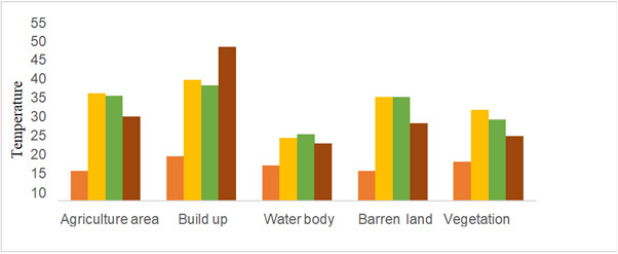

Figure 7: Mean LST for each LU/LC class during 1996-2017. **Note:** (■) 199 (■) 6; (■) 200; (■) 301.

The changing of the LST caused by LS changes since each type of land has its qualities in terms of energy radiation and absorption. Built-up (settlement) lands possess less albedo as well as higher absorption than barren lands due to the surrounding areas/barren lands having higher temperatures than urban areas. These outcomes conform to the researchers who found that areas with bare soil and build-up areas show a higher LST while other classification, such as water bodies, cultivate and vegetation, have lower LST values during sunlight. In contrast, during the night build up and barren lands have less LST values, while water bodies and vegetation found to have lesser LST value.

Land surface temperature and NDVI

Enhance the area of green cover along with green spaces in urban ecosystem has a major influence on the thermal condition of cities and expansion of UHI. Vegetation cover through evapotranspiration progression can reduce with adjust the temperature of the land surface. That is why in many of the studies conducted to find solutions to deal with the phenomenon and mitigate its effects; the function of green cover consider as one of the most significant behaviour to reduce the effects of UHI. The spatial pattern of LST and NDVI in the study display in Figure 6. At the time of the study, the NDVI value in Tehran varied between 0.15 and 0.34. Areas with the lowest NDVI value mainly spread in north-west, south, and south-west of Delhi (Figures 8 and 9).

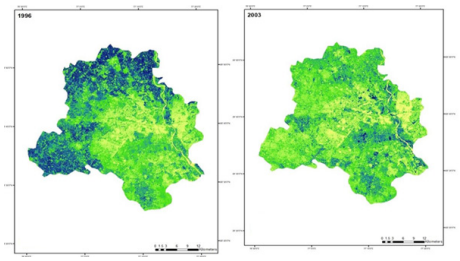

Figure 8: NDVI of the study area for the years 1996, 2003.

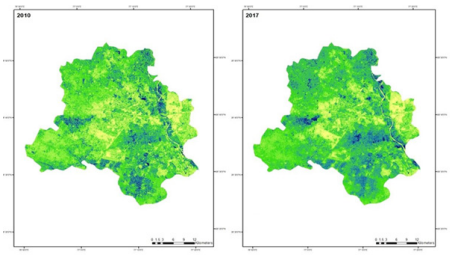

Figure 9: NDVI of the study area for the years 2010 and 2017(April).

The spatial yearly pattern of land surface temperature and NDVI in this case study display in Figure 6. At the time of the study, the NDVI value in Tehran varied between 0.15 and 0.34. Areas by the less NDVI value mostly spread in west, north, south west and east part of the city. The LST always influenced by water availability and green cover and also, there is a direct positive relationship between temperature, as well as material and coating of the surface. In this study, a total number of 500 points selected randomly to study the relationship between LST and NDVI in the form of a two-dimensional scatter plot in Figure 10.

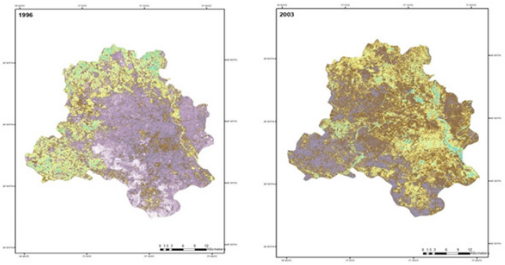

Figure 10: NDBI within each LU/LC class in1996, 2003.

The LST and NDVI exhibit opposite spatial distribution patterns. At the macro level, the areas with high LST values show the urban heat island phenomenon. These areas have relatively low NDVI values. At the micro-level, the high peaks of LST present a low valley of NDVI. In addition to a negative correlation between NDVI and LST, a negative relationship between LST and NDVI-derived green cover fraction exposed in the marks (Figure7) of the linear relationship, with the correlation coefficients of R^2=0.10 (1996), R^2=0.20 (2010) and R^2= 0.12 (2010) and R^2=0.5 (2017) which lower temperatures in vegetation area due to processes such as transpiration and evapotranspiration. It means that the higher the NDVI, the lower the LST and the higher the land surface temperature, the lower in NDVI.

Land surface temperature and NDBI

Normalised Difference Built-up Index (NDBI) image (Figure 6) shows a reverse pattern to the NDVI index in the sense that agriculture and other vegetated areas with high NDVI values showed low NDBI values. Likewise, build up (settlement) areas with low NDVI received high NDBI value. The lowest NDBI values are possessed by water while the highest value possessed by fallow land. In general, build up areas contain higher reflectance with reference to MIR band and is thus expected to have higher NDBI values but some studies show that reflectance for certain classes of vegetation cover increases as water content decreases . The drier vegetation cover can even have higher reflectance to MIR, resulting in higher Normalized Difference Built-up indicator. So, considering dry vegetation in the barren ground in upper hills and probably due to soil characteristics in low land, bare soil areas exhibit higher NDBI principles. Figure 8 present a high NDBI in 1996 and after that gradually decreased from the central part of the city to surrounding areas on 2003, 2010 and 2017. The area with the highest NDBI values appeared in the edges in 1996, which represent the agriculture and vegetation cover on 2003, 2010 and 2017 this time and less NDBI principles be able to be observed concentrated primarily in the essential part at centre of Delhi on 1996 and slowly spread which corresponds to the Build-up area on surrounding area and edges on Delhi on 2003, 2010 and 2017 (Figure 11).

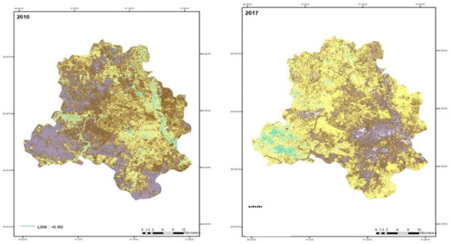

Figure 11: NDBI within each LU/LC class in 2010 and 2017(April).

Figure 8 shows the graph of the mean normalised difference built-up index within each land use and land cover class for 1996, 2003, 2010 and 2017. It can digitally see that Build up area has been transferring slowly from the central part of the city (1996) to surrounding areas in the city (2010 and 2017). In general, the NDBI values are high for build-up area in LU/LC classes for each year 1996, 2003, 2010 and 2017. Water has the lowest NDBI value (-0.3). After water, vegetation cover and agriculture have low NDBI values (-0.2). The barren land area also shows quite low NDBI value (0 to 0.1). On the other hand, build-up on LU/LC classes has substantially high NDBI values ranging from 0.4 (Figure 12).

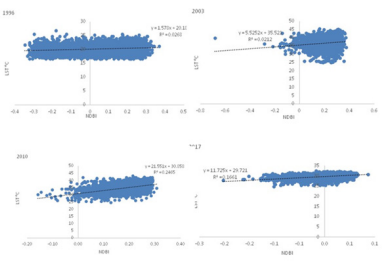

Figure 12: Correlation between NDBI and LST in the period of the study (1996, 2003, 2010 and 2017)

In fact, there is a positive correlation between NDBI and LST was shown in the results of the linear relationship, with the correlation coefficients of R^2=0.02 (1996), R2=0.02 (2003) and R^2=0.246 (2010) and R^2=0.16 (2017) (Figure 9). The linear relationship results detected a strong correlation between NDBI and LST, with correlation coefficients of R^2=0.26 in 2017. It is a positive correlation concerning physical changes, ground surfaces, and increased build-up areas in the barren land areas, which has a great effect on the heating of the ground surface (Figure 13).

Mapping urban heat islands (UHI)

As a result of interannual variation and different atmospheric conditions within the same period among years; it was not appropriate to compare multiple data images from different years. Th erefore, to compare LST from different d ates, a n ormalisation m ethod w as performed using the following equation. UHI monitoring was carried out on summer 1996- 2017 with 4 images of the Landsat. Figure 10 shows the UHI maps of 1996-2017.

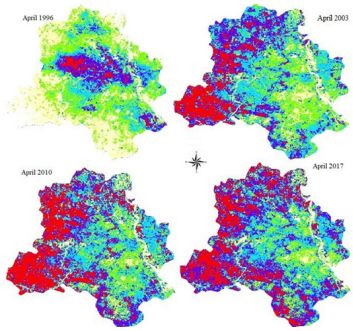

Figure 13: Urban heat island over April (1996-2017).

Figure 10 shows the central part of Delhi facing low temperature because of high density of green cover, because this large green protected areas, from heat trapping in the city and sub- urban areas across Delhi have high temperature because of high rocky lands and growing build up areas. Generally, earth objects reflect more energy than water bodies and green substances. The very high heat island observed over the suburb regions due to the presence of high-density residential areas and crop burning during the summer season. Furthermore, water bodies and vegetation object show fragile urban heat island intensity, observed throughout this Figures 10. Our results demonstrated that suburban areas of the Delhi city, rather than the central parts, are more influenced by UHI effects. The suburbs of Delhi are characterised by sparse vegetation cover and the barren rocky and agricultural areas. In the April 1996-2017 periods, the shapes of the UHI patterns are almost concentric, and the UHI values are increasing from the outskirts towards the inner areas. A large deviation from this shape occurs in the north-western part of the city, where the red colours towards the suburbs. This can be explained by the effect of large burning crops areas at summer season and with the high built-up ratio at suburb areas. In the whole investigated period the greatest UHI intensity (1.8 in April 2003 and 1.9 in April 2017) are found in the central cell.

Conclusion

This study is approved to recognise the environmentally significant areas based on LST, NDWI and NDBI to UHI expansion in Delhi. This study is mostly focusing on the connection between LST, NDBI and NDVI indices using Landsat 5, 7 and 8 images. Normalised difference built-up index and normalised difference vegetation index shows a positive correlation with land surface temperature. This study could observe that the LST has increased over the years from 1996 till 2017 on some specific areas where there is more anthropogenic activities happen and for the build-up areas (settlements and industrial areas). Evaluations of land surface temperature provide significant contribution for UHI restoration initiatives. Based on the results, it has been concentration, frequency of heat island occurring, and period of UHI, on the other hand, the climatic events under different climate change scenarios. This research shows sub-district UHI; therefore, highest heat stress needs particular attention. Regardless of the growth of green after sometimes cause urban heat island focus. In difference vegetation areas known as green which is very vital for sustainable urban planning.

References

1. Ahmed B, Kamruzzaman MD, Zhu X, Rahman MS, Choi K (2013) Simulating land cover changes and their impacts on land surface temperature in Dhaka, Bangladesh. Remote Sens 5: 5969-5998.
2. Abutaleb K, Adeline N, Ahmed F, Ahmed M, Elkafrawy S, et al. (2014) Investigation of urban heat island using Landsat data. In Proceedings of the 10th International Conference of AARSE 223.
3. Cibula WG, Zetka EF, Rickman DL (1992) Response of thematic bands to plant water stress. Int J Remote Sens 13: 1869-1880.
4. Corburn J (2009) Cities, climate change and urban heat island mitigation: localising global environmental science. Urban Studies 46: 413–427.
5. Deng C, Wu C (2013) Examining the impacts of urban biophysical compositions on surface urban heat island: A spectral unmixing and thermal mixing approach. Remote Sens Environ 131:262–274.
6. Dimoudi A, Zoras S, Kantzioura A, Stogiannou X, Kosmopoulos P, et al. (2014) Use of cool materials and other bioclimatic interventions in outdoor places in order to mitigate the urban heat island in a medium size city in Greece. Sustain Cities Soc 13:89-96
7. Hoverter SP (2012) Adapting to urban heat: a tool kit for local governments. Georgetown Climate Center.
8. Gao BC (1996) NDWI-A normalized difference water index for remote sensing of vegetation liquid water from space. Remote Sens Environ 58: 257-266.
9. Hall FG, Strebel DE, Nickeson JE (1991) Radiometric rectification: Toward a common radiometric response among multidate, multisensor images. Remote Sens Environ 35: 11-27
10. Giannopoulou K, Livada I, Santamouris M, Saliari M, Assimakopoulos M, et al. (2011) On the characteristics of the summer urban heat island in Athens, Greece. Sustain cities soc 1: 16–28
11. Li F, Jackson TJ, Kustas WP, Schmugge TJ, French AN, et al.(2004) Deriving land surface temperature from Landsat 5 and 7 during SMEX02/SMACEX. Remote sensing of environment 92: 521-534.
12. Li H, Liu Q (2008) Comparison of NDBI and NDVI as indicators of surface urban heat island effect in MODIS imagery. In International conference on earth observation data processing and analysis (ICEODPA) International Society for Optics and Photonics.
13. Raynolds MK, Comiso JC, Walker DA, Verbyla D(2008) Relationship between satellite-derived land surface temperatures, arctic vegetation types and NDVI. Remote Sensing of Environment 112: 1884–1894.
14. Rizwan AM, Dennis LY, Chunho LIU (2008) A review on the generation, determination and mitigation of urban heat island. J Environ Sci 20: 120–128.
15. Mallick J, Hang H, Rahman A, Abul Hasan M, Falqi I, et al. (2020) Assessing inter-seasonal variations of vegetation cover and land surface temperature in the ncr using Modis data. Appl Ecol Env Res 18: 4241-4258.
16. Morad M, Chalmers AI, Oregan PR (1996) The role of root-mean-square error in the geo-transformation of images in GIS. Int J Geogr Inf Sci 10: 347–353.
17. Mushore TD, Odindi J, Dube T, Mutanga O (2017) Understanding the relationship between urban outdoor temperatures and indoor air-conditioning energy demand in Zimbabwe. Sustain Cities Soc 34: 97–108.

18. Kuang MY, Huang Y (2010) Coupling urbanization analyses for studying urban thermal environment and its interplay with biophysical parameters based on TM/ETM+ imagery. Int J Appl Earth Obs Geoinf 12: 110-118.

19. Rouse JW, Haas RH, Schell JA, Deering DW (1973) Monitoring vegetation systems in the Great Plains with ERTS, Third ERTS Symposium, NASA SP-351 309- 317.

20. Şahin M (2012) Modelling of air temperature using remote sensing and artificial neural network in Turkey. Adv Space Res 50:973-985.

21. Song C, Woodcock CE, Seto KC, Lenney MP, Macomber SA (2001) Classification and change detection using Landsat TM data: When and how to correct atmospheric effects? Remote Sensing of Environment 75: 230–244.

22. Serrano L, Filella I, Penuelas J (2000) Remote sensing of biomass and yield of winter wheat under different nitrogen supplies. Crop Science 40: 723–731.

23. Schott JR, Volchok WJ (1985) Thematic mapper thermal infrared calibration. Photogram. Eng Rem Sens 51: 1351–1357. [GoogleScholar]

24. Shwetha HR, Kumar DN (2016) Prediction of High Spatio-Temporal Resolution Land Surface Temperature under Cloudy Conditions using Microwave Vegetation Index and ANN. ISPRS J Photogramm Remote Sens 117: 40-55.

25. Unger J, Sumeghy Z, Zoboki J (2001) Temperature cross section features in an urban area. Atmos Res 58: 117–127

26. Sobrino JA, Jiménez-Muñoz JC (2003) Land surface temperature retrieval from LANDSAT TM 5. Remote Sens Environ 90: 434-440

27. Yuan F, Bauer ME (2007)Comparison of impervious surface area and normalized difference vegetation index as indicators of surface urban heat island effects in Landsat imagery. Remote Sens Environ 106: 375–386.

28. Taha H (2015) Meteorological, air-quality, and emission-equivalence impacts of urban heat island control in California. Sustain cities soc 19: 207–221.

29. Tran DX, Pla F, Latorre-Carmona P, Myint SW, Caetano M, et al. (2017) Characterizing the relationship between land use land cover change and land surface temperature. ISPRS 132-133.

30. Weng Q, Lu D, Schubring J (2004) Estimation of land surface temperature–vegetation abundance relationship for urban heat island studies. Remote Sens Environ 89: 467–483.

31. Wukelic GE, Gibbons DE, Martucci LM, Foote HP (1989) Radiometric calibration of Landsat Thematic Mapper thermal band. Rem Sens Environ 28: 339–347.

32. Yue W, Xu J, Tan W, Xu L (2007) The relationship between land surface temperature and NDVI with remote sensing: application to Shanghai Landsat 7 ETM+ data. Int J Remote Sens 28: 3205–3226.

33. Zha, Yong Ni S, Yang S (2003). An effective approach to automatically extract urban land- use from TM imagery. J REM SENS BEIJ 7: 37-40.

34. Zinzi M, Agnoli S (2012) Cool and green roofs: an energy and comfort comparison between passive cooling and mitigation urban heat island techniques for residential buildings in the Mediterranean region. Energy Build 55: 66–76.